PRAMANA
— journal of
physics

© Indian Academy of Sciences

Vol. 73, No. 6
December 2009
pp. 969–988

Quasi-bound states, resonance tunnelling, and tunnelling times generated by twin symmetric barriers

A UMA MAHESWARI*, P PREMA, S MAHADEVAN and C S SHASTRY
Department of Sciences, Amrita Vishwa Vidyapeetham, Ettimadai, Coimbatore 641 105, India
*Corresponding author. E-mail: a_umamaheswari@ettimadai.amrita.edu

MS received 18 October 2008; revised 14 February 2009; accepted 26 June 2009

Abstract. In analogy with the definition of resonant or quasi-bound states used in three-dimensional quantal scattering, we define the quasi-bound states that occur in one-dimensional transmission generated by twin symmetric potential barriers and evaluate their energies and widths using two typical examples: (i) twin rectangular barrier and (ii) twin Gaussian-type barrier. The energies at which reflectionless transmission occurs correspond to these states and the widths of the transmission peaks are also the same as those of quasi-bound states. We compare the behaviour of the magnitude of wave functions of quasi-bound states with those for bound states and with the above-barrier state wave function. We deduce a Breit–Wigner-type resonance formula which neatly describes the variation of transmission coefficient as a function of energy at below-barrier energies. Similar formula with additional empirical term explains approximately the peaks of transmission coefficients at above-barrier energies as well. Further, we study the variation of tunnelling time as a function of energy and compare the same with transmission, reflection time and Breit–Wigner delay time around a quasi-bound state energy. We also find that tunnelling time is of the same order of magnitude as lifetime of the quasi-bound state, but somewhat larger.

Keywords. Twin symmetric barrier; quasi-bound states; resonant tunnelling.

PACS Nos 03.65.-w; 03.65.Xp

1. Introduction

Over the last several years the subject of resonant tunnelling has become an area of detailed study as can be seen from a representative list of references [1–8]. This is partly due to its importance in areas like nanoscience and electronic devices. In general, in non-relativistic quantum mechanics the resonance phenomena can be related to the comparatively long-lived positive energy states. When they have very narrow widths, they are often referred to as quasi-bound (QB) states. Resonant process is a well-investigated area in three-dimensional (3D) quantal scattering

which has facilitated a clear understanding of resonance reactions in atomic and nuclear collision processes. In the same spirit, in the analysis of resonance tunnelling it is important to define clearly a QB state associated with one-dimensional (1D) quantal tunnelling problems and relate them to the behaviour of the corresponding reflection coefficient R and transmission coefficient T and in particular to the positions and widths of peaks occurring in T. It is also important to relate the commonly defined tunnelling time T_q to the lifetime of the corresponding QB state. We undertake this study in this paper and obtain our conclusions based on two explicit examples of resonance tunnelling across symmetrically placed twin barriers in one dimension.

The non-relativistic quantal theory of 3D potential scattering provides a unified analysis of bound states below the threshold energy $E = 0$ and continuum above the threshold [9–15]. The bound states are fully normalizable negative energy states; however, above the threshold the regular radial wave functions for positive energy behave like $\sin(kr - l\pi/2 + \delta_l)$ for large r, where δ_l is the partial wave phase shift. These phase shifts generate corresponding partial wave differential cross-sections which, depending on the nature of the scattering potential, may generate sharply peaked oscillations in the cross-sections as a function of energy. These are attributed to resonance generated by the scattering potential. A resonance state for a given partial wave is characterized by its energy $E_r > 0$ and width $\Gamma_r > 0$. The theory of potential scattering in 3D visualizes such a state as an eigenstate with complex energy eigenvalue $E_R = E_r - i\Gamma_r/2$. In contrast with the bound state energy $E = -E_\mathrm{b}$, the resonance state is strictly speaking not normalizable and diverges asymptotically exponentially as a function of r but decreases as $\mathrm{e}^{[-\Gamma_r t/(2\hbar)]}$ with time and has lifetime $\tau = \hbar/\Gamma_r$. In fact, a resonance scattering is a time-delayed process. However, if the width is narrow the behaviour of the resonance wave function within the interaction region is very similar to that of the infinitely long-lived bound state and picks up its radial divergence slowly well outside the interaction region.

In general, in 3D scattering the sharp resonance states are generated by a potential having a pocket followed by a barrier at energies below the barrier height. In fact, the counterparts of such states in classical scattering are strictly bound. Hence it is appropriate to use the term quasi-bound (QB) states for these sharp resonances. Analytic S-matrix (SM) theory of potential scattering [9–15] provides a unified picture of bound states and resonances in terms of the pole structure of partial wave SM. Evaluations of such states are very important in areas like nuclear scattering and decay of unstable nuclei via alpha decay, proton emission etc. as evident from refs [14–19]. A detailed procedure exists for the study of such states in 3D scattering theory. It is in this context that in this paper we study the QB states generated in one-dimensional transmission problems. However, the counterpart of scattering cross-section in 1D transmission problems are T and R which manifest in their variation as a function of E the existence of QB states in 1D. Hence we need to clearly define these states in 1D transmission problems parallel to complex energy eigenstates in 3D scattering.

Recent work of Rakityansky [4] deals in detail with the computation of bound states and resonances in 1D. In this paper we deal with a specific case of transmission across symmetric twin barriers with the specific objective of studying the

nature of QB states, resonance transmission and tunnelling time in order to demonstrate various interesting features. The use of symmetrical barriers substantially simplifies the computation. In conformity with some similar earlier investigations [7] we find that T across such twin barriers shows sharp resonance peaks at energies below the barrier height. We find that positions and widths of these peaks correspond to the complex eigenvalues of the QB states defined in our study. Clearly at such resonance energies $R = 1 - T$ shows a dip indicating practically zero reflection [20]. Using an approximate spectral representation for the full resolvent operator associated with 1D Lippmann–Schwinger (LS) equation we are able to establish that indeed peaks of T in resonance tunnelling generated by QB states can be described by a sum of Breit–Wigner (BW) type terms containing resonance energy positions and widths.

The evaluation of T above the barrier height also generates well-spaced comparatively broader peaks. The study of resonances in 3D scattering has confirmed the existence of the above-barrier resonances. In the same spirit the above-barrier peaks of T in the case of 1D tunnelling are correlated with broad above-barrier resonance states dominating the barrier domain and therefore should not be labelled as QB state. Interestingly, however, we found that T above the barrier height in the domain of barrier resonances can also be approximately described by a suitably altered empirical BW-type formula.

Another interesting feature that we investigated is the variation of T_q, transmission time T_{qt} and reflection time T_{qr} as a function of energy, in particular around the positions of QB states. We find that T_{qt} and T_q show sharp peaks at the resonance positions confirming that resonance tunnelling is indeed a time-delayed transmission in the QB states. At resonance positions $T_{qt} \gg T_{qr}$ and further that T_q is somewhat higher but has the same order as the lifetime of the QB state. These variations of T_q, T_{qt} and T_{qr} show similar behaviour in the vicinity of each resonance. We also compare the BW delay time $\tau_{\rm BW}$, with T_q, T_{qt} and T_{qr}.

The plan of the paper is as follows: In §2 using the results of 3D scattering we define the QB state associated with the transmission across one-dimensional symmetrically placed twin barrier and summarize the numerical results for a set of two model potentials together with the study of the behaviour of the magnitude of the wave functions. In §3 we study the resonance structure generated by T and formulate multilevel BW-type formula to describe the same. Section 4 contains a comparative study of T_q, T_{qt}, T_{qr}, $\tau_{\rm BW}$ and the lifetime τ associated with the QB states. Section 5 summarizes the main conclusions.

2. Formulation

We formulate the study of QB states and resonance tunnelling in one dimension by suitably modifying the corresponding procedure in 3D for s-wave. The modified radial Schrödinger equation for the wave function $u(r)$ satisfies the differential equation

$$\frac{\mathrm{d}^2u(r)}{\mathrm{d}r^2} + (k^2 - V(r))u(r) = 0. \tag{1}$$

Here $k^2 = 2mE/\hbar^2$ and $V(r) = 2mU(r)/\hbar^2$. In the unit of convention $\hbar^2 = 2m = 1$, the terms k^2 and $V(r)$ have dimension L^{-2} and represent energy and potential, respectively. Unless otherwise stated in our numerical calculations we adopt the unit Å for length and energy is expressed in Å^{-2}. $R(r) = u(r)/r$ is the radial solution. The regular solution $u(r)$ of eq. (1) satisfies the initial condition

$$u(r) \underset{r\to 0}{\longrightarrow} O(r). \tag{2}$$

The solution $u(r)$ can also be expressed as a linear combination of two irregular solutions (also known as Jost solutions) $f(k,r)$ and $f(-k,r)$ satisfying the asymptotic conditions

$$f(\pm k, r) \underset{r\to\infty}{\longrightarrow} \mathrm{e}^{\mp ikr}. \tag{3}$$

Thus one writes $u(r)$ as

$$u(r) = \frac{1}{2ik}[F(-k)f(k,r) - F(k)f(-k,r)]. \tag{4}$$

The coefficients $F(\pm k)$ are known as Jost functions and are given by Wronskian

$$F(\pm k) = W[u(r), f(\pm k, r)]. \tag{5}$$

The Jost functions are independent of r and hence can be calculated at any convenient point $r = R$ where scattering potential is negligible. The s-wave S-matrix (SM) is given by

$$S(k) = \mathrm{e}^{2i\delta(k)} = \frac{F(k)}{F(-k)}, \tag{6}$$

where $\delta(k)$ is the s-wave phase shift. The power of analytic SM theory lies in the fact that for a wide range of potentials the bound states and resonant states can be identified with certain type of poles of $S(k)$ generated by the zeros of $F(-k)$ in the complex k-plane. For example, the zero of $F(-k)$ occurring at $k = ik_b$ on the positive imaginary axis corresponds to a bound state regular solution $u(r)$ decreasing asymptotically as $\mathrm{e}^{-k_b r}$ and hence normalizable. The corresponding energy eigenvalue $E = -k_b^2$. Similarly, consider a zero at $k = k_r - ik_i$ of $F(-k)$ in the lower half of complex k-plane which gives rise to a pole in the S-matrix. When $k_i \ll k_r$, this corresponds to a resonant state with positive resonance energy E_r and width Γ_r:

$$E_r = k_r^2 - k_i^2, \tag{7}$$

$$\Gamma_r = 4k_r k_i. \tag{8}$$

Thus, in the complex E plane the SM has a pole at $E_R = E_r - i\Gamma_r/2 = E_r - iE_i$. The width Γ_r, expressed in energy units, is related to decay constant λ, mean life τ and half-life $\tau_{1/2}$ through the relation

$$\frac{1}{\lambda} = \tau = \frac{\tau_{1/2}}{0.693} = \frac{\hbar}{\Gamma_r}. \tag{9}$$

At resonance, the wave function $u(r)$ varies asymptotically as $e^{ik_r r}e^{k_i r}$ for large r and the time variation of the corresponding time-dependent part of the wave function is $e^{-iE_r t}e^{-t\Gamma_r/2}$ indicating a positive energy QB state with finite lifetime. Inside the potential pocket and barrier region, the QB state wave function behaves very similar to the bound state wave function [21]. This is illustrated in §3. The term $e^{k_i r}$ represents the fact that decaying state asymptotically diverges as a function of r. Thus, the resonant state wave function is not normalizable in the entire radial domain. It is important to note that solution $u(r)$ of Schrödinger eq. (1) which is regular at origin and behaves like an outgoing wave e^{ikr} as $r \to \infty$, is possible only when $k_i > 0$. This is because, when k is real, $F(\pm k) \neq 0$ and $|S(k)| = 1$. This means, for real k, $u(r)$ has both incoming and outgoing wave components. However, at the pole position $k = k_r - ik_i$, with k_i very close to zero, $u(r)$ inside the interaction region will be real for all practical purposes. For real potentials the zeros of $F(\pm k)$ are symmetric with respect to imaginary k-axis. This is a consequence of the symmetry relation satisfied by Jost functions (see ref. [9], pp. 338–340)

$$F(k) = F^*(-k^*). \tag{10}$$

Intuitively speaking, this symmetry is a consequence of the fact that $e^{ikr} = [e^{-ik^*r}]^*$ which is a property satisfied by Jost solution $f(\pm k, r)$ also. This means that if $k = k_p = k_r - ik_i$ is a pole of $S(k)$, then $k = -k_p^* = -k_r - ik_i$ is also a pole. However, the pole at $k = -k_p^*$ has no additional significance. In fact the states corresponding to $k = k_p$ and $k = -k_p^*$ are time reversal states of each other. Similarly, the symmetry relation of eq. (10) further implies that if k_p is a pole of the SM, k_p^* is a zero of the same. In the vicinity of sharp resonance, incorporating dominant poles and zeros, the resonating term of the SM can be written as

$$S = \frac{(k + k_p)(k - k_p^*)}{(k - k_p)(k + k_p^*)}. \tag{11}$$

This expression, which also satisfies the unitarity property of the SM, governs the resonance dominance in the s-wave scattering cross-section, and in the vicinity of resonance leads to the standard BW formula for s-wave cross-section

$$\sigma_s = \frac{\pi}{k^2}\frac{\Gamma_r^2}{(E - E_r)^2 + \Gamma_r^2/4}.$$

In the light of these 3D results, in the case of 1D we deal with a potential which is symmetric with respect to the origin having two barriers on either side. Thus the 1D Schrödinger equation is

$$\frac{d^2\Psi(x)}{dx^2} + (k^2 - V(x))\Psi(x) = 0, \tag{12}$$

where $V(x) = V(|x|)$. Such a potential, if sufficiently attractive, in general can generate bound states which have either symmetric or antisymmetric wave functions decreasing exponentially as $|x| \to \infty$. It is well-known that the antisymmetric negative parity solutions of eq. (1) [22] necessarily cross origin and hence in the domain $x \geq 0$ are nothing but the corresponding bound state eigenfunctions for

the 3D s-wave problem for the potential $V(r) = V(x)$, $x \geq r$ described by eq. (1). In analogy with the 3D case, the QB or resonant states of the 1D problem with potential $V(|x|)$ have the asymptotic behaviour given by

$$\Psi(x) \xrightarrow[x\to\infty]{} \mathrm{e}^{i(k_r - ik_i)x}, \tag{13}$$

$$\Psi(x) \xrightarrow[x\to-\infty]{} \mathrm{e}^{-i(k_r - ik_i)x}. \tag{14}$$

These conditions imply that the state decays on either side of the barrier.

As in the 3D case $\Psi(x)$ will diverge exponentially for large x and will decay in time as $\mathrm{e}^{-\Gamma_r t/2}$. Hence the computation of 1D QB state with complex energy E_R requires numerical solution of the Schrödinger equation satisfying the boundary conditions (eqs (13) and (14)). For well-behaved potentials $V(|x|)$ and near the origin, 1D symmetric QB state behaves as a cosine function and as a sine function in the case of antisymmetric state. Since we are dealing with the symmetric potential the computation of the wave function can be carried out restricting to the domain $x > 0$ and solutions for $x < 0$ can be obtained using symmetry properties. For our study we consider two different double barrier symmetric potentials:

(i) Twin rectangular barrier:

$$\begin{aligned} &V(x) = 0, \quad |x| < a, \\ &V(x) = V_0 > 0, \quad a < |x| < b, \\ &V(x) = 0, \quad |x| > b. \end{aligned} \tag{15}$$

The corresponding potential for 3D case is

$$\begin{aligned} &V(r) = 0, \quad 0 < r < a, \\ &V(r) = V_0, \quad a \leq r \leq b, \\ &V(r) = 0, \quad r > b. \end{aligned} \tag{16}$$

(ii) Twin Gaussian barrier:

$$V(x) = V_0 \mathrm{e}^{[-(|x|-a)^2/c^2]}, \quad 0 \leq |x| \leq \infty, \quad V_0 > 0 \tag{17}$$

and the corresponding potential for 3D case is

$$V(r) = V_0 \mathrm{e}^{[-(r-a)^2/c^2]}, \quad r \geq 0. \tag{18}$$

In tables 1 and 2 we list the complex momenta and complex energy of the resonant states obtained using the potential given by eq. (15) for the cases of two different sets of potential parameters. As expected the width of the barrier drastically alters the imaginary part, but real part changes only marginally. The states indicated by (*) are occurring at above-barrier energies and we do not treat them as QB states. They can be designated as above-barrier resonant states [23–25]. In table 2 the resonances are listed over a wider range of energy since these are used for further analysis in the next section. For comparison we also list the bound state energies generated by the potential

Table 1. The list of resonance states generated for a symmetric twin barrier potential $V(x)$ given by eq. (15) with parameters $V_0 = 8$, $a = 3$, $b = 4.5$. The states indicated by the (*) are the first two above-barrier states, still higher states are not listed.

Quantum number n	$k = k_r - ik_i$	$k^2 = (k_r^2 - k_i^2) - i2k_rk_i$ $= E_r - i\Gamma_r/2$	Parity
0	0.468, $-i$0.737e-5	0.219, $-i$0.690e-5	+
1	0.935, $-i$0.384e-4	0.874, $-i$0.718e-4	−
2	1.398, $-i$0.136e-3	1.955, $-i$0.380e-3	+
3	1.856, $-i$0.468e-3	3.444, $-i$0.174e-2	−
4	2.302, $-i$0.180e-2	5.298, $-i$0.829e-2	+
5	2.724, $-i$0.818e-2	7.421, $-i$0.446e-1	−
6	3.094, $-i$0.389e-1	9.571, $-i$0.241*	+
7	3.361, $-i$0.118	11.281, $-i$0.794*	−

Table 2. The list of resonance states generated for a symmetric twin barrier potential $V(x)$ given by eq. (15) with parameters $V_0 = 8$, $a = 3$, $b = 3.5$. The states indicated by the (*) are the above-barrier states. All states up to $k^2 = 21.5$ are listed. The resonance parameters obtained here are used in the numerical computation of T described in the text.

Quantum number n	$k = k_r - ik_i$	$k^2 = (k_r^2 - k_i^2) - i2k_rk_i$ $= E_r - i\Gamma_r/2$	Parity
0	0.462, $-i$0.210e-2	0.214, $-i$0.194e-2	+
1	0.925, $-i$0.845e-2	0.855, $-i$0.156e-1	−
2	1.387, $-i$0.192e-1	1.924, $-i$0.532e-1	+
3	1.850, $-i$0.344e-1	3.422, $-i$0.127	−
4	2.314, $-i$0.542e-1	5.351, $-i$0.251	+
5	2.778, $-i$0.787e-1	7.712, $-i$0.437	−
6	3.243, $-i$0.108	10.508, $-i$0.701*	+
7	3.709, $-i$0.142	13.740, $-i$1.056*	−
8	4.176, $-i$0.182	17.406, $-i$1.520*	+
9	4.642, $-i$0.228	21.496, $-i$2.113*	−

$$V(x) = 0, \quad |x| < a$$
$$V(x) = V_0, \quad |x| > a \tag{19}$$

and these are listed in table 3 and can be treated as the limiting cases of QB states when barrier width $(b - a) \to \infty$. In figures 1 and 2 we also show the comparative variation of the magnitude of typical bound state and QB state wave functions in interaction region for two typical cases. The similarity in the behaviour of the QB and bound state wave functions gives ample justification for treatment of QB states as bound states in many practical applications [21,26,27]. The very slow rise of $|\Psi|$ for QB state when $|x|$ increases is due to the small imaginary part k_i.

In table 4 we give the results for resonant states obtained for the potential given by eq. (17). The nature of these results is similar to those obtained from eq. (15) and discussed earlier. These are also used in the study of T described in §3.

Table 3. The list of bound states generated for a symmetric rectangular well $V(x)$ given by eq. (19) with parameters $V_0 = 8$, $a = 3$. These should be compared with the QB state results listed in tables 1 and 2.

Quantum number n	k	k^2	Parity
0	$0.468i$	0.219	+
1	$0.935i$	0.874	−
2	$1.398i$	1.956	+
3	$1.856i$	3.444	−
4	$2.301i$	5.296	+
5	$2.713i$	7.363	−

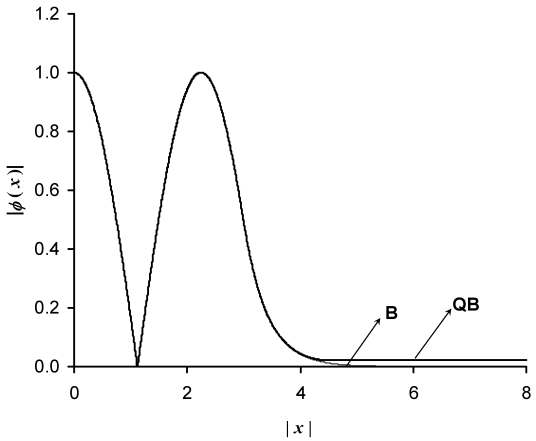

Figure 1. Comparative study of the magnitude of symmetric wave function of the bound state (B) ($k = 1.398$, $k^2 = 1.955$) and QB state ($k = 1.398 - i0.136e\text{-}03$, $k^2 = 1.955 - i0.380e\text{-}03$) in the interaction region of the potential given by eq. (15). Potential parameters are $V_0 = 8$, $a = 3$, $b = 4.5$.

3. Multi-level formula for sub-barrier T

In order to obtain T and R in one-dimensional transmission problem, one solves the 1D Schrödinger eq. (12) satisfying the asymptotic conditions

$$\Psi(x) \xrightarrow[x\to-\infty]{} A\mathrm{e}^{ikx} + B\mathrm{e}^{-ikx}$$
$$\Psi(x) \xrightarrow[x\to\infty]{} F\mathrm{e}^{ikx} \tag{20}$$

such that $T = |F/A|^2$ and $R = |B/A|^2$. We first study T and R as functions of energy for the potential given by eq. (17) with parameters $V_0 = 8$, $a = 3$, $c = 0.3$. We have taken this case having smaller barrier width so that resonances become reasonably broad for graphical analysis. In figure 3 we show the variation of T as a function of energy in the energy range $E = 0$–16. It is very clear that at

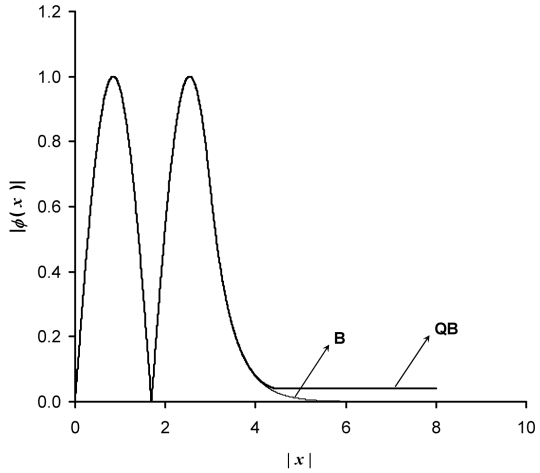

Figure 2. Comparative study of the magnitude of antisymmetric wave function of the bound state (B) ($k = 1.856$, $k^2 = 3.444$) and the QB state ($k = 1.856 - i0.468e\text{-}03$, $k^2 = 3.444 - i0.174e\text{-}02$) in the interaction region of the potential given by eq. (15). Potential parameters are $V_0 = 8$, $a = 3$, $b = 4.5$.

below-barrier energies the peaks in T and the corresponding dips in R occur precisely at the energies of QB states and we have verified that the halfwidths of these peaks are the same as that computed from the imaginary part of the complex eigenenergy of QB states. We have obtained similar results in the case of potential of eq. (15) with potential parameters $V_0 = 8$, $a = 3$ and $b = 3.5$. These results establish that reflectionless transmission for the symmetric twin barrier occurs at the energies of QB states and the width of the peak of T corresponds to the width of the QB state. The peaks in figure 3 at $E > 8$ correspond to the above-barrier resonances which have larger widths.

It is tempting to examine whether the variation of T at sub-barrier energies seen in figure 3 can be fully explained in terms of QB state energies and widths. We investigate this using reasonable approximations and obtain an expression for T as a function of energy below the barrier valid in the case of resonance tunnelling. The problem of transmission and reflection can be studied in terms of the LS equation (see ref. [9], p. 181) which is nothing but the integral equation corresponding to the Schrödinger equation. The LS equation for the full tunnelling state $|\Psi\rangle$ is given by

$$|\Psi\rangle = |\Phi\rangle + GV|\Phi\rangle. \tag{21}$$

Here $|\Phi\rangle$ is the incident state, V is the barrier and $G = (E - H)^{-1}$ is the full resolvent operator. $H = H_0 + V$ is the full Hamiltonian. Thus, in configuration space $\langle x|\Phi\rangle$ is the incident wave function and $\langle x|\Psi\rangle = \Psi(x)$ is the full solution satisfying eq. (20). In general, the operator G can be expressed as a spectral representation involving discrete bound states and continuum states (see ref. [9], p. 184). For the purpose of our present analysis, we assume that it is reasonable to approximate G at

Table 4. The list of QB states generated for a symmetric twin Gaussian barrier potential $V(x)$ given by eq. (17) with parameters $V_0 = 8$, $a = 3$, $c = 0.3$. The resonance parameters obtained here are used in the numerical computation of T described in the text.

Quantum number n	Resonance position in k-plane $k = k_r - ik_i$	Resonance position in E-plane $k^2 = (k_r^2 - k_i^2) - i2k_rk_i$	Parity
0	0.511, $-i$0.188e-2	0.261, $-i$0.192e-2	+
1	1.020, $-i$0.813e-2	1.040, $-i$0.166e-1	−
2	1.524, $-i$0.205e-1	2.321, $-i$0.626e-1	+
3	2.022, $-i$0.417e-1	4.086, $-i$0.169	−
4	2.516, $-i$0.741e-1	6.323, $-i$0.373	+

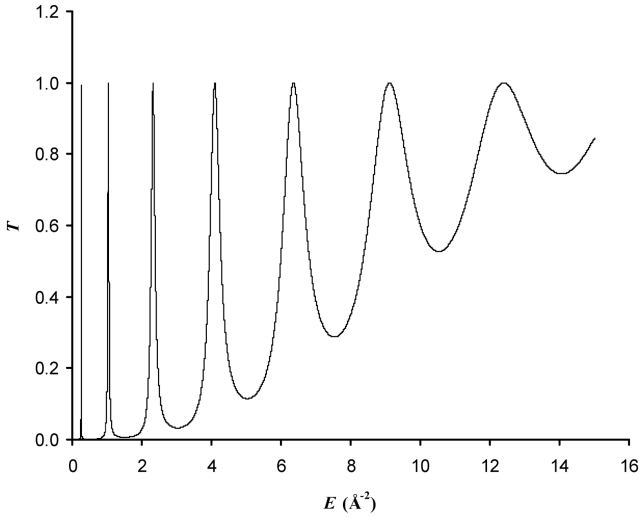

Figure 3. Variation of T as a function of energy E for the potential given by eq. (17). Potential parameters are $V_0 = 8$, $a = 3$, $c = 0.3$. The peaks of T indicate the QB states and above-barrier resonances.

below-barrier energy in terms of spectral representation using adequately normalized well-separated QB states $|\phi_n\rangle$ confined to the interaction domain. Thus we write

$$G = \sum_n \frac{|\phi_n\rangle\langle\phi_n|}{E - E_n}. \tag{22}$$

The state $|\phi_n\rangle$ has complex energy eigenvalue $E_n = E_{nr} - i\Gamma_{nr}/2$ and obeys the boundary conditions of eqs (13) and (14). Substituting eq. (22) in eq. (21) we get

$$|\Psi\rangle \approx |\Phi\rangle + \sum \frac{|\phi_n\rangle\langle\phi_n|V|\Phi\rangle}{(E - E_n)}. \tag{23}$$

Using

$$\langle\phi_n|V|\Phi\rangle = \langle\phi_n|H - H_0|\Phi\rangle = (E_n - E)\langle\phi_n|\Phi\rangle \tag{24}$$

and expanding $|\Phi\rangle = \sum C_n|\phi_n\rangle$ with $C_n = \langle\phi_n|\Phi\rangle$ and after some simplification one gets

$$|\Psi\rangle = \sum \frac{C_n(i\Gamma_{nr})}{(E - E_{nr}) + i\Gamma_{nr}/2}. \tag{25}$$

Since $|\Phi\rangle$ represents a plane wave moving from $-\infty$ to $+\infty$ and $|\phi_n\rangle$ is a QB state which propagates on either side of the interaction region towards $\pm\infty$, it is reasonable to assume that near the resonance energy $C_n \approx 1/2$. Thus in the vicinity of resonance, T will be dominated by the BW-type expression (see for example ref. [9], p. 596). Hence the BW-type formula for T is

$$T = \frac{(\Gamma_{nr}^2/4)}{(E - E_{nr})^2 + \Gamma_{nr}^2/4}. \tag{26}$$

Clearly, eq. (26) gives $T = 1$ at $E = E_{nr}$. This signifies reflectionless transmission shown in figures 4 and 5 and indicates that approximations used are appropriate. In the case of sufficiently well N separated narrow QB states, neglecting cross terms one can write T as

$$T = \sum_{n=1}^{N} \frac{(\Gamma_{nr}^2/4)}{(E - E_{nr})^2 + \Gamma_{nr}^2/4}. \tag{27}$$

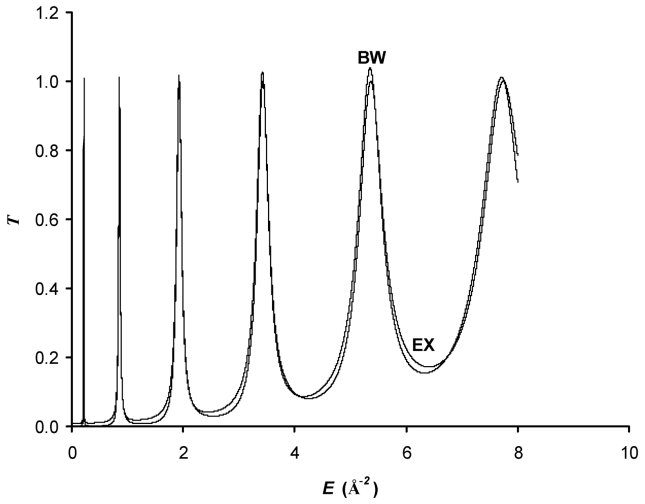

Figure 4. Comparison of the variation of T as a function of energy E generated by BW-type formula given by eq. (27) with the exact T (EX) obtained from numerical computation. The potential used is given by eq. (15). The potential parameters are $V_0 = 8$, $a = 3$, $b = 3.5$. The peaks of T indicate the QB states.

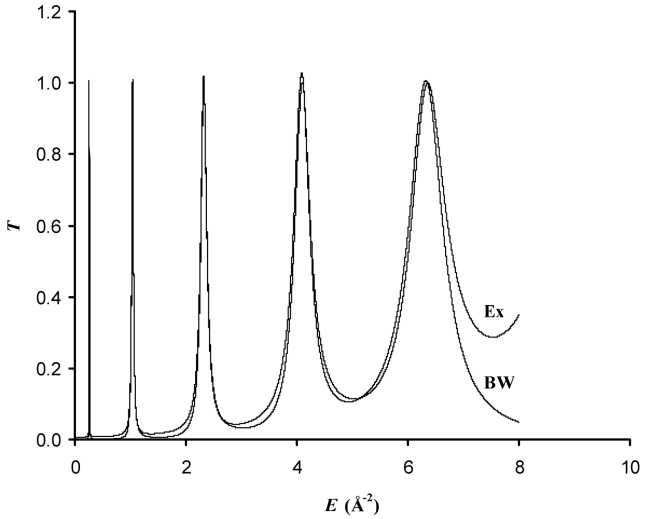

Figure 5. Comparison of the variation of T as a function of energy E generated by BW-type formula (27) with the exact T (EX) obtained from numerical computation. The potential used is given by eq. (17). The potential parameters are $V_0 = 8$, $a = 3$, $c = 0.3$. The peaks of T indicate the QB states.

Using our computed energy eigenvalues E_{nr} and Γ_{nr} in the expression for T we have computed T at below-barrier energies and compared it with the variation of exact T in the same domain. In figure 4 we show the results obtained for rectangular twin symmetric barrier given by eq. (15) and corresponding to the QB state data listed in table 2. One finds that the BW-type multilevel formula (eq. (27)) for T fits remarkably well with the variation of T as a function of energy below the barrier. These results demonstrate that at below-barrier energies T is dominated by resonances. We have repeated these calculations in the case of continuous potential given by eq. (17) and results are shown in figure 5 further confirming the success of eq. (27) in describing T quite well at below-barrier energies.

In order to explore this method further, we have computed T for energies above the barrier up to $E = 23$ for the potential given by eq. (15). In figure 6 we show the results. As stated earlier, these above-barrier peaks are also a kind of resonance peaks. These are the counterparts of the broad above-barrier states in 3D scattering referred earlier. The complex energy eigenvalues corresponding to these peaks are listed in table 2. However, these states should not be treated on par with the QB states. In order to illustrate this, in figure 7 we show a comparison of the variation of the magnitude of a typical QB state and an above-barrier state wave function. The former, like a bound state, damps inside the barrier whereas the latter picks up amplitude at the barrier. This justifies the term 'above-barrier resonances'. These are comparatively broad and their width decreases with the increase of barrier width. Further, at the positions of these peaks, transmission is not reflectionless, though R is quite small. In view of this and also due to the overlapping behaviour of these broad states, the BW-type formula (eq. (27)) was found too inadequate to describe T at above-barrier energy. While attempting to fit the above-barrier T we

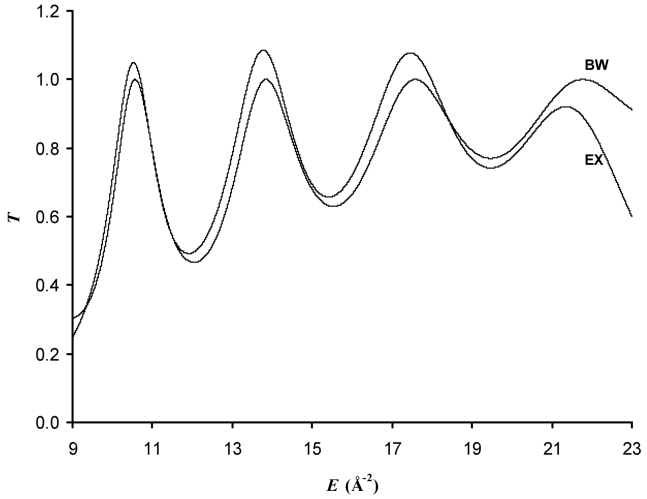

Figure 6. Comparison of the variation of exact T (EX) and the T (BW) obtained from the empirical formula given by eq. (28) with energy E at the above-barrier energies for the potential given by eq. (15). The potential parameters are $V_0 = 8$, $a = 3$, $b = 3.5$.

found the inclusion of damping factor $\mathrm{e}^{-2(b-a)k_{ni}}$ in BW-type formula, resulting in the expression

$$T = \sum_{n=1}^{N} \frac{(\Gamma_{nr}^2/4)\mathrm{e}^{-2(b-a)k_{ni}}}{(E - E_{nr})^2 + \Gamma_{nr}^2/4} \tag{28}$$

can be fruitfully used to schematically describe the variation of T at above-barrier energies in terms of barrier top resonance parameters and figure 6 includes these results. This damping factor is thought of as a kind of empirical renormalization factor bringing the description of T at above-barrier energies to a model similar to the formulation used for the below-barrier energies. Since this approach is purely empirical, we will not further elaborate on this.

4. Comparison of tunnelling time and decay time

In all tunnelling phenomena, the concept of tunnelling time is a well-studied topic [1,28–34]. However, relation between the tunnelling times and the decay time or mean lifetime $\tau = \hbar/\Gamma_r$ of QB states is not examined in detail in literature. To avoid intricacies involved in different concepts of tunnelling time in this paper we restrict to T_{qt}, T_{qr} and T_q as elaborated in ref. [1], pp. 352–356. According to this, T_q can be expressed as the sum of reflection time T_{qr} and transmission time T_{qt}. Denoting the phases of complex amplitudes B and F by ϕ_r and ϕ_t respectively, the quantal tunnelling time T_q is defined as

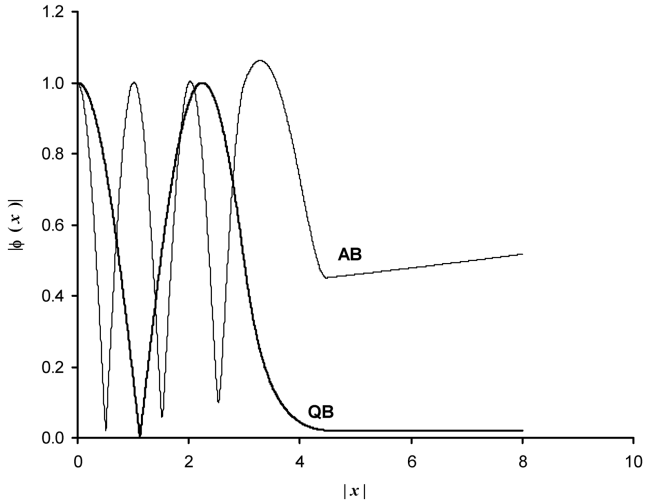

Figure 7. The variation of magnitude of the wave function of typical QB state ($k^2 = 1.955 - i0.380e\text{-}03$) with that of the above-barrier (AB) resonant state ($k^2 = 9.571 - i0.241$) for the potential given by eq. (15). The potential parameters are $V_0 = 8$, $a = 3$, $b = 4.5$.

Table 5. Numerical results for T_{qr}, T_{qt} and T_q in seconds at QB state energies (eV) for electron tunnelling obtained for the potential of eq. (15) with parameters $V_0 = 8$, $a = 3$, $b = 3.5$.

E_r (eV)	E_i (eV)	T_{qr} (s)	T_{qt} (s)	T_q (s)	τ (s)
0.817	7.420e-03	1.216e-17	7.133e-14	7.135e-14	4.431e-14
3.263	5.966e-02	6.120e-18	1.030e-14	1.031e-14	5.511e-15
7.342	2.027e-01	4.545e-18	2.861e-15	2.866e-15	1.622e-15
13.058	4.852e-01	2.452e-18	1.086e-15	1.088e-15	6.777e-16
20.419	9.568e-01	1.906e-18	4.822e-16	4.841e-16	3.437e-16
29.429	1.669	1.137e-18	2.339e-16	2.351e-16	1.970e-16

$$T_q = \frac{m}{\hbar k}\left[R\frac{\mathrm{d}\phi_r}{\mathrm{d}k} + T\frac{\mathrm{d}\phi_t}{\mathrm{d}k}\right] = T_{qr} + T_{qt}. \tag{29}$$

In figures 8 and 9 we show the variation of T_{qt} as a function of energy at below-barrier energies for the symmetric rectangular twin barrier given by eq. (15). It is clear that the position of peaks of T_{qt} occur at the QB state energies confirming that QB states are time-delayed states. We have repeated this calculation for the smooth potential given by eq. (17) showing similar trend. In tables 5 and 6 we have listed the numerical values of τ, T_{qr}, T_{qt} and T_q corresponding to QB state energies in the case of potentials given by eqs (15) and (17). For better comprehension of the results, we have converted the results for the tunnelling of electrons and listed the results in eV and seconds. The unit of length used is Å. Conversion factors are: The time τ (in seconds) $= 1.7234e\text{-}16/\Gamma$ (in Å^{-2}) and Γ (eV) $= 3.816\times[\Gamma$ (in Å^{-2})].

Table 6. Numerical results for T_{qr}, T_{qt} and T_q in seconds at QB state energies (eV) for electron tunnelling obtained for the potential of eq. (17) with parameters $V_0 = 8$, $a = 3$, $b = 0.3$.

E_r (eV)	E_i (eV)	T_{qr} (s)	T_{qt} (s)	T_q (s)	τ (s)
9.971e-1	7.331e-03	1.953e-16	6.868e-14	6.888e-14	4.486e-14
3.969	6.327e-02	2.637e-18	9.765e-15	9.767e-15	5.197e-15
8.857	2.388e-01	5.077e-18	2.433e-15	2.437e-15	1.377e-15
15.590	6.438e-01	3.661e-18	7.974e-16	8.010e-16	5.108e-16
24.130	1.423	2.471e-18	2.971e-16	2.997e-16	2.310e-16

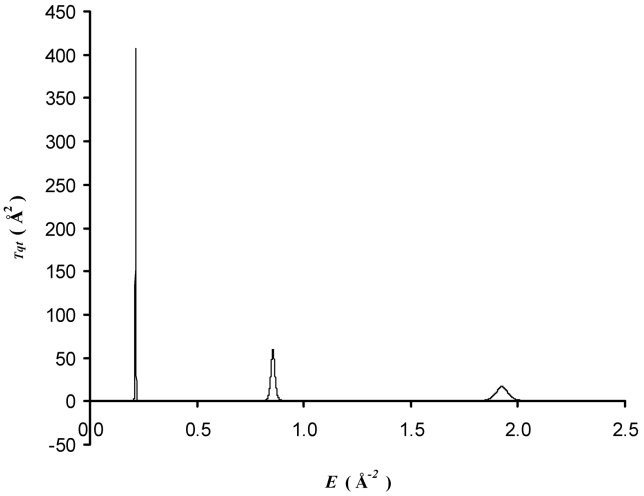

Figure 8. Variation of T_{qt} as a function of below-barrier energy E(0–2.5) shows peaks at QB state energies for the potential given by eq. (15). The potential parameters are $V_0 = 8, a = 3, b = 3.5$.

Thus if $V_0 = 8$ Å^{-2}, the height of the barrier is 30.528 eV. These results show that at QB state energies $T_{qr} \ll T_{qt}$. Further, T_{qt} is smaller than T_q but both have the same order of magnitude. This difference between τ and T_q should not be surprising because the lifetime τ of QB state is related to the possible decay of the QB state with equal probability on either side of the twin barriers whereas tunnelling time is defined with respect to a situation composed of incident wave, reflected wave on one side and transmitted wave on another side given by eq. (20). Thus, one may say that this difference in τ and T_q is primarily due to the difference in boundary conditions used for QB state and transmission problem. Further, the dominance of T at resonance makes T_{qt} practically the same as T_q and T_{qr} small. Therefore, it is of interest to study the variation of T_q, T_{qr} and T_{qt} in more detail in the vicinity of QB energies. In figures 10–12 we show a typical set of results. It is seen that the difference between T_q and T_{qt} increases as one move away from QB state energy but they have similar functional behaviour which shows a Lorentzian-type behaviour [30] and is not unexpected. On the other hand, T_{qr} variation is quite different and

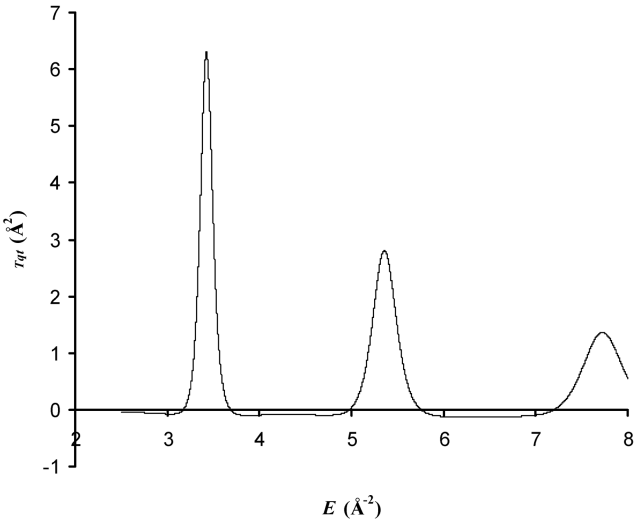

Figure 9. Variation of T_{qt} as a function of below-barrier energy $E(2.5–8.0)$ shows peaks at QB state energies for the potential given by eq. (15). The potential parameters are $V_0 = 8, a = 3, b = 3.5$.

has qualitative behaviour similar to that of $|\mathrm{d}T_q/\mathrm{d}(k^2)|$. This is easily visualized from figures 10–12. In addition, in figure 11, in order to demonstrate a relative behaviour of various time-scales T_{qr}, T_{qt}, T_q and τ_{BW} we have included the result for the time delay $\tau_{\mathrm{BW}}(E)$ given by the BW-type formula

$$\tau_{\mathrm{BW}}(E) = \frac{(\Gamma_{nr})}{(E - E_{nr})^2 + \Gamma_{nr}^2/4}. \tag{30}$$

Clearly, the above definition implies that at $E = E_{nr}$, $\tau_{\mathrm{BW}} = 2\tau$. Thus, the numerical results obtained in this and earlier sections of the paper clearly bring out various facets of the resonance tunnelling across symmetric twin barrier.

5. Conclusions

The results described in this paper give a comprehensive picture of resonance tunnelling in 1D by a symmetric twin barrier and provide a correlation with the 3D resonance scattering by spherically symmetric potential. With this knowledge of the general nature of the results, one can use more general techniques [4] for the study of more complicated tunnelling problems. The main conclusions of this paper can be summarized as follows:

1. We have studied the resonance tunnelling across a symmetrically placed twin barrier using two specific cases involving rectangular barriers and Gaussian barriers respectively. We find that the positions of peaks and widths of T as a function of energy correspond to the position and widths of QB states

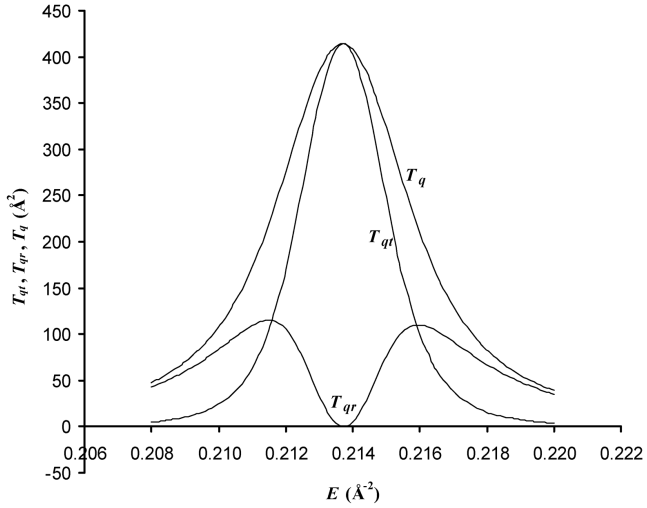

Figure 10. Variation of T_q, T_{qr}, T_{qt} with E in the vicinity of the first QB state energy ($E_R = 0.214 - i0.194e\text{-}02$) for the potential given by eq. (15). The potential parameters are $V_0 = 8, a = 3, b = 3.5$.

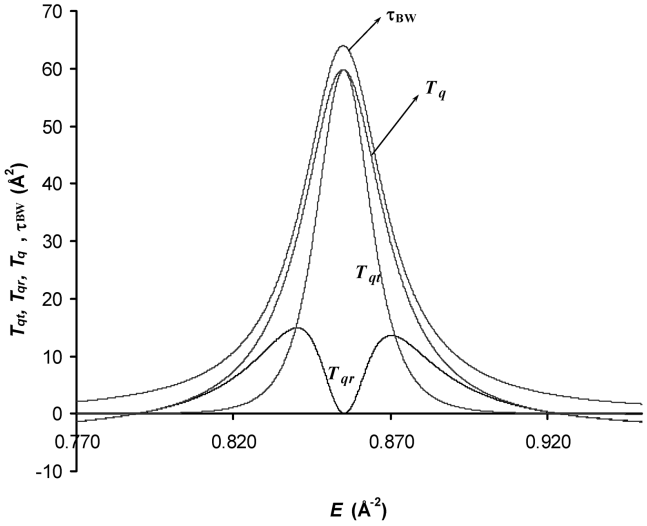

Figure 11. Variation of T_q, T_{qr}, T_{qt} and τ_{BW} with E in the vicinity of second QB state energy ($E_R = 0.855 - i0.156e\text{-}01$) for the potential given by eqs (15) and (30) gives the definition of τ_{BW}. The potential parameters are $V_0 = 8, a = 3, b = 3.5$.

generated by the pocket formed by the two barriers. These QB states behave similar to the corresponding bound states within the interaction domain, but outside they gradually grow exponentially with increase in $|x|$ but decay in time characterized by the mean lifetime $\tau = \hbar/\Gamma$. On the other hand, unlike

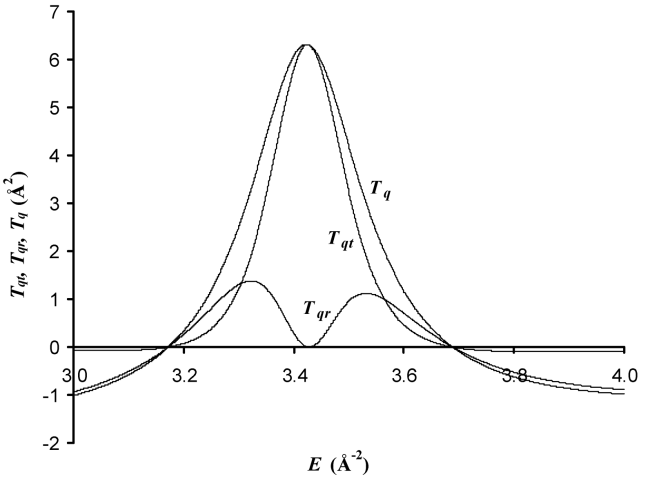

Figure 12. Variation of T_q, T_{qr}, T_{qt} with E in the vicinity of fourth QB state energy ($E_R = 3.422 - i0.127$) for the potential given by eq. (15). The potential parameters are $V_0 = 8, a = 3, b = 3.5$.

QB states the above-barrier resonance states have dominance around the barrier region and are broader.

2. In the tunnelling situation, the resonances in the transmission correspond to decay of the QB states predominantly through the transmission channel and at QB energies it is a reflectionless transmission. The variation of T at below-barrier energies can be well explained in terms of BW-type formula containing the QB state parameters. This formula is deduced heuristically using the QB state-based spectral representation of the full resolvent operator G governing the LS equation for tunnelling problem. At the above-barrier energies, the broad peaks are associated with the above-barrier resonances but they do not generate reflectionless transmission. The variation of T at the above-barrier energies also can be approximately fitted using empirically modified BW-type terms. We believe, that the pattern of results obtained here will be valid even for the case of transmission across equispaced multiple barriers generating well-separated QB states.
3. The variation of total tunnelling time T_q shows conspicuous peaks at QB state energies. T_q and the QB state lifetime τ are of the same order of magnitude but the latter is significantly smaller. We attribute this to the different boundary conditions satisfied by QB state and wave function describing the tunnelling.
4. In the vicinity of a QB state, both T_q and transmission time T_{qt} are quite close to each other and behave similarly around resonance domain but reflection time T_{qr} is much smaller and has quite a different behaviour. All these variations are approximately symmetric with respect to the energy of the QB state. In particular T_q and T_{qt} show Lorentzian-type behaviour, but somewhat differs from the strictly Lorentzian behaviour of τ_{BW}.

Acknowledgement

One of the authors (C S Shastry) acknowledges the financial support from Department of Science and Technology, Government of India in the form of a research grant (Project No. SR/S2/HEP-18/2004-II).

References

[1] Mohsan Razavy, *Quantum theory of tunnelling* (World Scientific, Singapore, 2003)
[2] M C Goorden, Ph Jacquod and J Weiss, *Phys. Rev. Lett.* **PRL100**, 067001 (2008)
[3] V S Olkhovsky, E Recami and G Selesi, *Euro. Phys. Lett.* **57**, 879 (2002)
[4] S A Rakityansky, *Phys. Rev.* **B68**, 195320 (2003)
[5] A P Barbero, H E Hernandez-Figueroa and E Recami, *Phys. Rev.* **E62**, 8628 (2000)
[6] E F P Lyngdoh, I Jamir and C S Shastry, *Phys. Educ.* (ISSN 0970-5953) **15**, 145 (1998)
[7] S Mahadevan, A Uma Maheswari, P Prema and C S Shastry, *Phys. Educ.* (ISSN 0970-5953) **23**, 13 (2006)
[8] S Mahadevan, P Prema, S K Agarwalla, B Sahu and C S Shastry, *Pramana – J. Phys.* **67**, 401 (2006)
[9] R G Newton, *Scattering theory of waves and particles* (McGraw Hill, New York, 1966)
[10] J R Taylor, *Scattering theory: The quantum theory on non-relativistic collisions* (John Wiley, New York, 1972)
[11] V De Alfero and T Regge, *Potential scattering* (North Holland, Amsterdam, 1965)
[12] C J Jochain, *Quantum collision theory* (North Holland, Amsterdam, 1975)
[13] S K Agarwalla, G S Mallick, P Prema, S Mahadevan, B Sahu and C S Shastry, *J. Phys. G: Nucl. Part. Phys.* **32**, 165 (2006)
[14] S Mahadevan, P Prema, C S Shastry and Y K Gambhir, *Phys. Rev.* **C74**, 057601 (2006)
[15] P Prema, S Mahadevan, C S Shastry, A Bhagawat and Y K Ghambir, *Int. J. Mod. Phys.* **E17**, 1 (2008)
[16] C Xu and Z Ren, *Nucl. Phys.* **A753**, 174 (2005)
[17] T Sil, S K Patra, B K Sharma, M Centelles and X Vinas, *Phys. Rev.* **C69**, 044315 (2004)
[18] V Y Denisov and H Ikezoe, *Phys. Rev.* **C72**, 064613 (2005)
[19] P R Chowdhury, C Samanta and D N Basu, *Phys. Rev.* **C73**, 014612 (2006)
D N Basu, *Phys. Rev.* **C66**, 027601 (2002)
[20] C Pacher, arXiv:quant-ph/0607027 2 (2007)
[21] E Maglione, L S Ferreira and R J Liotta, *Phys. Rev. Lett.* **81**, 538 (1998)
[22] B Sahu, M Z Rehman Khan, C S Shastry, B Dey and S C Phatak, *Am. J. Phys.* **57**, 886 (1989)
[23] W A Freidman and C J Goebel, *Ann. Phys.* **104**, 145 (1997)
[24] D M Brink, *Semiclassical methods in nucleus–nucleus scattering* (Cambridge University Press, Cambridge, 1965)
[25] P Susan, B Sahu, B M Jywra and C S Shastry, *J. Phys. G: Nucl. Part. Phys.* **20**, 1243 (1994)
[26] C N Davids and H Esbensen, *Phys. Rev.* **C61**, 054302 (2000)
[27] S Aberg, P B Semmes and W Nazarewicz, *Phys. Rev.* **C56**, 1762 (1997); *Phys. Rev.* **C58**, 3011 (1998)

[28] E H Hauge, J P Falck and T A Fjeldly, *Phys. Rev.* **B36**, 4203 (1987)
[29] C R. Leavens and G C Aers, *Phys. Rev.* **B39**, 1202 (1989)
[30] F Steinbach, A Ossipov, Tsampikos Kottos and T Geisel, *Phys. Rev. Lett.* **85**, 4426 (2000)
[31] Chun-Fang Li and Qi Wang, *Physica* **B296**, 356 (2001)
[32] S Li, S Kočinac and V Milanović, *Phys. Lett.* **A372**, 191 (2008)
[33] Chun-Fang Li and Harald Spieker, *Opt. Commun.* (ISSN 0030-4018), **259**, 158 (2006)
[34] Mark R A Shegelski, Jeremy Kavka and Jeff Hnybida, *Am. J. Phys.* **75**, 504 (2007)